INTERNATIONAL
Agrophysics
www.international-agrophysics.org

Int. Agrophys., 2023, 37, 201-214
doi: 10.31545/intagr/162959

Study of the pore structure characteristics of soybean grain piles using image processing technology

Mengmeng Ge, Guixiang Chen, Chaosai Liu, Deqian Zheng, and Wenlei Liu*

College of Civil Engineering, Henan University of Technology, Zhengzhou 450001, China

Received February 20, 2023; accepted April 3, 2023

A b s t r a c t. Pore structure is an important factor affecting the airflow distribution in a grain pile, and hence the variation in its structural parameters under different vertical pressures should be studied further. In this study, grain slice imaging and image processing technologies were comprehensively used to study the changes in the number, size, and shape of the pores in soybean grain piles under vertical pressures of 0, 50, 100, 150, 200, 250, and 300 kPa, and to explore the effects of vertical pressure on the porosity, pore volume, pore diameter, and pore fractal dimension of the grain piles. The results show that the porosity of the grain pile decreased with an increase in the vertical pressure, and the change rate of grain pile porosity was 28% when the vertical pressure was 0-300 kPa. When the vertical pressure increased from 50 to 300 kPa, the grain pile porosity variation increased from 6.49 to 24.33% as compared with the natural state (0 kPa). The pore area and diameter of the grain pile gradually decreased with the increase in vertical pressure. The distribution of the grain pile pore area along the horizontal direction from the side wall to centre showed great differences under different vertical pressures. With an increase in vertical pressure, the proportion of the pore diameter of < 2.5 mm increased, whereas the proportion of the pore diameter of > 2.5 mm decreased. An increase in the vertical pressure will lead to an increase in the grain pile pore fractal dimension. When the vertical pressure was 0-300 kPa, the change rate of the grain pile pore fractal dimension was 10%. The relevant research methods and conclusions drawn in this study may be used to provide theoretical support and a reference source for the airflow distribution and resistance changes in the bulk grain piles.

K e y w o r d s: soybean grain pile, vertical pressure, pore structure, image processing technology

INTRODUCTION

Food security is crucial for both national economic development and social stability. The temperature and moisture distribution in the grain pile changes due to variations in the environment, grain respiration, and in microbial activity (Altuntas and Demirtola, 2007). When the grain temperature and moisture content in some areas of the grain pile exceeded a certain critical value for safe storage, the induction of grain mildew, disease, and pest damage occurs easily, this may affect the surrounding grain and pose a danger to grain storage safety (Wu *et al*., 2020). In order to effectively control the quality of the stored grain and prevent grain losses, it is necessary to understand the real-time temperature and moisture distribution in a storage grain pile. Based on these considerations, effective control measures, such as mechanical ventilation (Nwaizu and Zhang, 2021) and static storage, may be formulated. The mechanical ventilation of grain piles is an effective measure to ensure safe grain storage. A fan is used to circulate air that has a certain temperature and humidity into the grain pile and this serves to maintain the temperature and humidity of the grain within the recommended range in order to achieve safe grain storage. The complex and variable pore structure in the grain pile affects the ventilation airflow velocity, airflow direction, and stacking density (Amanlou and Zomorodian, 2011; Nalladurai *et al*., 2002;

*Corresponding author e-mail: cgx@haut.edu.cn

Yue and Zhang, 2017a), which causes changes in airflow resistance and further affects the ventilation efficiency of the grain (Tiusanen *et al*., 2013). Therefore, understanding the changes in the pore structure of the grain pile is very important in designing grain drying and ventilation systems and ensuring grain storage safety.

As is typical in a porous medium, grain piles have a non-uniform pore structure. Understanding its irregular structural characteristics is crucial for determining airflow resistance (Wojciech *et al*., 2012), predicting fluid transport in bulk solids (Yue and Zhang, 2017b), and verifying the mathematical model of drying, ventilation, and also the fumigation mode of the stored grain (Nwaizu and Zhang, 2021). Currently, most numerical models use spherical particles to approximate grain (Yue and Zhang, 2017b), but compared with spherical particles, a reduction in porosity and pore area caused by the shape of non-spherical particles will increase the pressure gradient in the grain pile and reduce air velocity (Hilton *et al*., 2010; Liu *et al*., 2008). Similarly, assuming that the pore structure of the bulk particles is simple, constant, and uniform may lead to an inaccurate prediction of the airflow velocity and pressure distribution in grain piles during ventilation (Khatchatourian and Savicki, 2004). Neethirajan *et al*. (2006) showed that the long axis of the grains tend to line up in the horizontal direction when they are stored, this produces the differences between the porosity values of the grain piles in the horizontal and vertical directions, and affects the distribution of air velocity and resistance. There are trillions of pores with different quantities of various sizes and shapes in bulk grain piles in large storage silos. The pressure exerted by the storage grain piles will cause changes to the structures of the pores (Liu *et al*., 2022d), this will lead to an uneven distribution of airflow during ventilation and an increase in airflow resistance (Chung *et al*., 2001) which lowers drying and ventilation efficiency, resulting in a higher temperature and moisture in the low airflow area, which could easily lead to local grain heating, mildew, diseases, and pests (Mohapatra *et al*., 2017; Narendran *et al*., 2019; Nourmohamadi-Moghadami *et al*., 2020a; Nourmohamadi-Moghadami *et al*., 2020b). Some researchers have shown that with an increase in vertical pressure, the grain density increased and porosity decreased (Cheng *et al*., 2017; Cheng *et al*., 2015). Compared with the calculated value of airflow resistance, as studied by Shedd (1951), and considering the influence of vertical pressure on porosity, Haque (2011) showed that a change in porosity would lead to increased airflow resistance. Currently, most of the numerical algorithms used to solve fluid flow problems in porous media just ignore various factors, these include the differences in particle shape, the complex dynamics of airflow in pores, and the changes in pore structure characteristics. Lawrence *et al*. (2013) simulated the airflow distribution in a grain pile using CFD Fluent, but the anisotropy of the particles was disregarded in the study. For the numerical simulation of the grain pile ventilation process, some studies attempt to take into account the change in pore structure characteristics. In considering the anisotropy of the bulk particles and assuming that the porosity changes linearly from the centre to the wall, some researchers (Lawrence and Maier, 2012; Olatunde *et al*., 2016; Panigrahi *et al*., 2020) have simulated and studied the distribution of airflow and static pressure in a storage grain pile, but neglected to take into account the influence of the vertical pressure of the grain pile on the geometric and morphological characteristics of the pore structure. The numerical calculation model above cannot possibly reflect the actual pore structure distribution of the grain particles, it is worth noting that the air velocity and resistance of the grain pile varies significantly according to the pore characteristics. Therefore, it is important to clarify the effect of different vertical pressures on the pore structure parameters of the grain piles.

The inherent heterogeneity and spatial variation in the arrangement of the pores increases the complexity of the study with regard to the internal pore structure of quantitative bulk grain piles (Neethirajan *et al*., 2006). Imaging technology has been widely used in the study of the pore structure of soil (Budhathoki *et al*., 2022; Hu *et al*., 2018), concrete (Tian and Han, 2018; Vicente *et al*., 2018; Yuan *et al*., 2018), and other materials (Vicente *et al*., 2019). For the purposes of grain research, Neethirajan *et al*. (2008) studied changes in grain pore structure using imaging and graphics processing technology and the results showed significant differences in both porosity and pore size distribution between wheat and pea. Yuan *et al*. (2016) conducted numerical simulation research concerning the drying process of corn grain piles, and found that the higher the grain porosity, the faster the grain dried, and the shorter the time required to reach the same moisture content. Chen *et al*. (2019) simulated the ventilation and the drying process of a storage grain pile based on the moisture and heat transfer model of a grain pile. The results showed that the pore structure of the grain pile had a great impact on the simulation results of the model. However, the influence of vertical pressure on the characteristics of the structure was disregarded in the above-mentioned studies on grain pore structure.

During the bulk storage of grain in large storage silos, the bulk density changes due to the weight of the grain load, this affects the pore structure of the bulk grain. Currently, the actual pore structure distribution of grain piles is being studied through experiments, and the influence of vertical pressure on pore structure parameters is low. Therefore, in order to focus on the issue of the influence of grain pile pressure on the changes to pore structure and taking a soybean pile unit in different configurations in a grain bin as the research object, a test device was designed in this study to measure the pore structure parameters of the soybean pile under vertical compression. Simultaneously, the

influence of vertical pressure change on the pore area, pore size, and fractal dimensions of the soybean grain pile were studied based on image processing technology by using resin to fix the pore space structure of the grain pile.

The purpose of this study was to create a method to quantitatively study the pore structure of bulk particles. Additionally, image processing technology was used to quantitatively characterize the number, size, and shape of the pores in soybean grain piles under different pressures, and then to study the influence of vertical pressure changes on the characteristics of the pore structure.

MATERIALS AND METHODS

In order to evaluate the effect of vertical pressure on grain pile pore structure, a test device was used, it was composed of a loading frame, test chamber, and measuring system, as shown in Fig. 1. The test chamber was made from an aluminium alloy and transparent plexiglass, it had a size of 120 ×120 × 55 mm. The vertical loading screw was located in the groove, and vertical pressure was evenly applied to the soybean grain pile through the loading plate, which can sustainably provide a pressure of 2 000 kPa. The extension length of the screw was determined by the height of the sample. A dial indicator was mounted on the loading screw in order to measure the compression data of the soybean grain pile under different vertical pressures. A setting screw was set on the platform to record the position of the cantilever.

The test sample in this study was the medium yellow 36# harvested in 2020, after the broken particles and foreign impurities had been filtered. According to the ASAE standard ((R2017), 2017), the initial moisture content of the soybean sample was 12.8 ± 0.1% (w.b.) after drying at 103°C for 72 h using the drying method as per manual. Equivalent diameter (D_p) is often used to describe the size of irregular objects. Sphericity (S_p) is used to indicate the difference between the actual shape of the particles and spherical particles. The larger the value, the more spherical the particle. Grain bulk and particle densities were determined according to the ASAE standard ((R2017ED), 2017). In order to determine the size characteristics of soybean particles, 100 particles were randomly selected to measure their triaxial size length, width, thickness, equivalent diameter, and sphericity using the following equations (Ghodki *et al*., 2019):

$$D_p = (L_p W_p T_p)^{1/3}, \quad (1)$$

$$S_p = (L_p W_p T_p)^{1/3} / L_p, \quad (2)$$

where: D_p is the equivalent diameter of the particles, S_p is the sphericity of the particles, and L_p, W_p, and T_p are the length, width, and thickness of the particles, respectively. Table 1 summarizes the physical properties of the soybean samples used in this study.

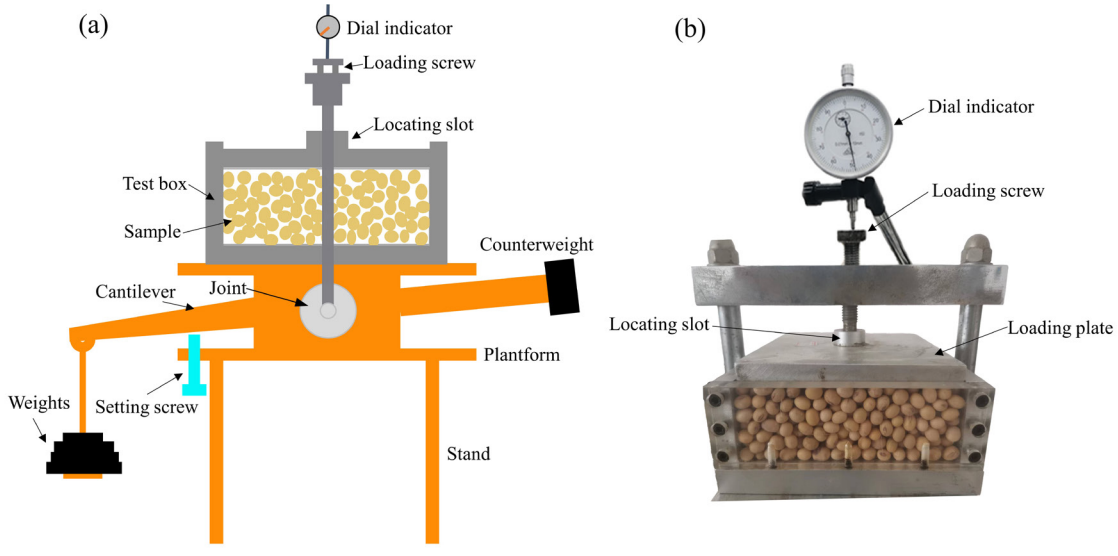

Fig. 1. Schematic diagram of the compression test device: a – test device and b – test chamber.

Table 1. Physical properties of the soybean grain sample

Moisture content (%)	9.73	Equivalent diameter (m)	7.27×10^{-2}
Average (m)			
length	8.56×10^{-2}	Sphericity	0.89
width	7.25×10^{-2}	Particle density (kg m^{-3})	1245
thickness	6.17×10^{-2}	Grain bulk density (kg m^{-3})	743

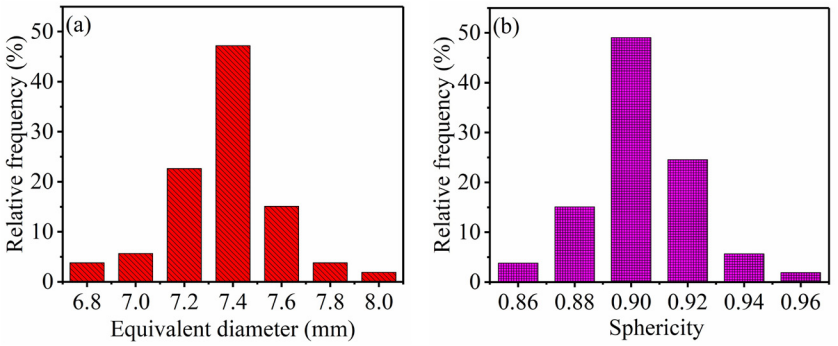

Fig. 2. Soybean particle size distribution: a – equivalent diameter and b – sphericity.

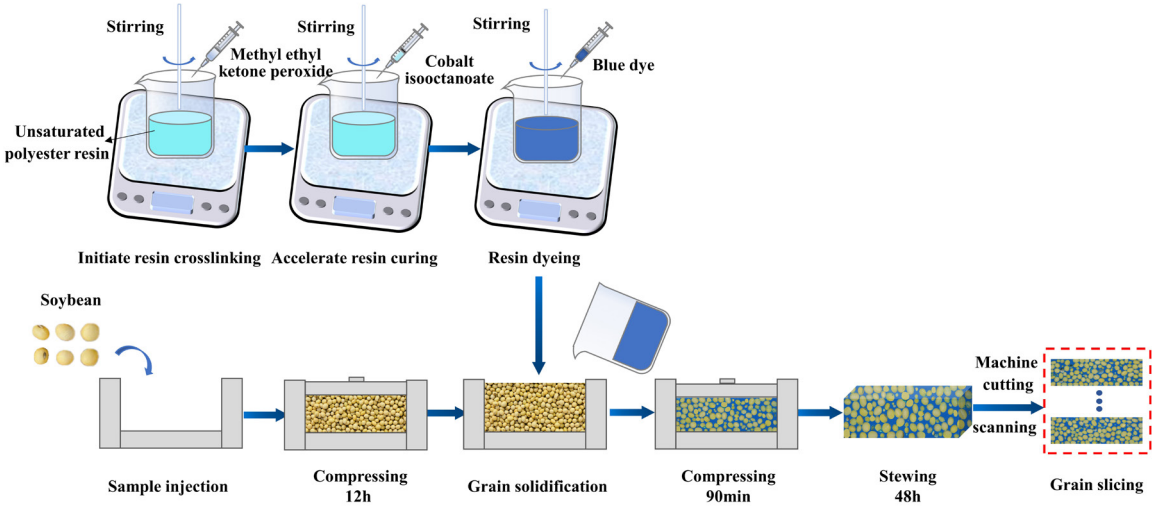

Fig. 3. Schematic diagram of the grain image acquisition test.

Figure 2a shows the distribution of the equivalent diameter of the soybean particles. The distribution range of the equivalent diameter of soybean particles was relatively narrow, and 85% of the size distribution lay within the range of 7.2-7.6 mm. Figure 2b shows the sphericity distribution of soybean granules. The sphericity distribution of soybean granules was also relatively concentrated, with most of its values being > 0.9.

Because the sample area in this study was different from the conventional consolidation meter test, the stress applied on the soybean was estimated in advance. After the calculation was performed, the applied vertical stress was 3, 8, 18, 28, 50, 75, 100, 125, 150, 200, 250, and 300 kPa (Liu *et al*., 2022a; 2022b; 2022c; 2022d). The soybean samples were loaded into the device through free fall addition, the grain surface was paved, and the average height of the sample, h, was recorded. In this study, the soybean samples were subjected to multistage loading at pressures of 0, 50, 100, 150, 200, 250, and 300 kPa. Each loading stage lasted for 20 min before the final stress level was reached. Thereafter, within the first hour after reaching a constant pressure loading, the measurement data were recorded after every five-minutes had elapsed, after that, measurements were performed every hour. The grain particles experienced creep under vertical pressure, and eventually reached a state of stability when the displacement change was < 0.2% of the total displacement. This test recorded the compression data for 12 h (Liu *et al*., 2022d). After the compression test reached a state of stability, the position of the cantilever was noted, this was used to solidify the grain pile under the same conditions. Simultaneously, the compression data h_i were measured under different vertical pressures, and the porosity value was calculated using Eq. (6) after each loading stage.

The pore structure of the soybean grain pile under different pressures was solidified to form a grain casting, and the grain image was processed by cutting. The process is shown in Fig. 3.

In this study, an unsaturated polyester resin curing system was used to cure the pore structure of the soybean pile, and the effect of vertical pressure on the change in the

pore structure parameters of the grain pile was studied. The specific steps involved in obtaining each grain pile slice image were as follows:

1. Selection of the curing method, resin, and curing agent. The test was performed at 10-30°C using the cold curing method, which is simple and convenient to execute, gelling is rapid, and it produces a good moulding effect. It is easy to soak the sample in and to cure unsaturated polyester resin. It is an excellent casting resin. The oxidation and reduction curing system of methyl ethyl ketone peroxide and cobalt isooctanoate was used in the test. Its curing was sufficient, the casting body was not too easy to break, and it had an excellent curing effect. The methyl ethyl ketone peroxide reacted with cobalt isooctanoate, releasing a large amount of heat, and promoting resin curing.

2. Preparation of the resin curing agent. First, the required amount of unsaturated polyester resin was injected into the preparation solution, methyl ethyl ketone peroxide was added, it was quickly stirred until completely mixed, and then cobalt isooctanoate was added. To easily distinguish between the skeleton particles and pores in the image, a special blue coloured paste was added to dye the resin. The amount of methyl ethyl ketone peroxide and cobalt isooctanoate was 2% of the weight of the resin, and the gelation time was 1 h. The resin was used as prepared. In addition, the direct reaction between methyl ethyl ketone peroxide and cobalt isooctanoate releases a lot of heat; therefore, direct contact between the two was avoided.

3. Grain pile solidification. A compression test of the soybean pile under different vertical pressures was conducted with the improved consolidation instrument. After measuring the compression data under different vertical pressures, the position of the compression rod was recorded. Thereafter, the loading plate was raised, the prepared resin curing agent was slowly injected along the inner wall of the compression container, and it was allowed to stand for 15 min so that the impregnating agent could fill the pores of the grain pile. After loading took place up to the recording position, the loading plate was kept stationary for 90 min. After the resin solidified, the grain pile casting was removed and allowed to rest for 48 h at 10-30°C. The steps above were repeated in order to obtain the grain pile casting under different pressures.

4. Grain pile slice image. Differences were noted in the pore structure parameters in different sections of the grain pile casting body. In this study, the average value of multiple sections were taken as the pore structure parameters of the grain pile under different vertical pressures. The resin grain casting was cut using machine tool (XD-40A) at a feed rate of 100 mm min^{-1}, and the sample slice image was obtained by scanning the casting using a BenQ 5560 scanner. A colour image is shown in Fig. 4a. The operation process was as follows: first, the grain casting body was fixed on the machine tool, a flat end face was milled to serve as the reference plane, the grain pile casting body was cut at five millimetre intervals along the horizontal direction, the casting body was removed after the plane cutting operation was completed, the section was scanned using a scanner, and half (6 cm) of the sample was taken along the horizontal direction for analysis and research, that is, 12 grain pile slice images were obtained for each sample. All of the images were resized to 2770 × 910 pixel images to include an area with vivid details of the pores across the section (Fig. 4).

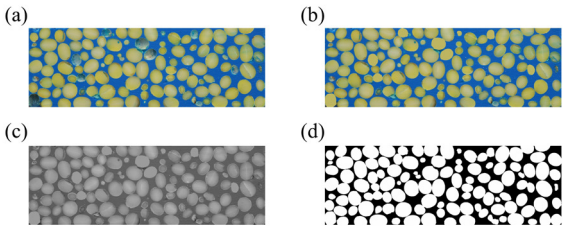

Fig. 4. Grain image binarization diagram: a – original image, b – patch image, c – grayscale image, and d – binary image.

In the process of cutting grain castings using a machine tool, the grain particles fell off the slice due to a high level of friction. The use of drawing software was necessary in order to fill in the missing particles. The patch image is shown in Fig. 4b. Accordingly, the image was processed through grayscale and binarization, and the process is shown in Fig. 4. Finally, Fiji/Image J software, image processing software that was developed by the United States National Institute of Health, was used to statistically analyse the grain and pore information in the image in order to study the changes in grain pile pore structure parameters.

The grain pile image obtained using the scanner was a coloured image, namely an RGB image. A pixel is represented by three two-dimensional (2D) arrays of the same size, and the three arrays represent three primary colour components. This kind of image data contains a large amount of information and is difficult to analyse and process. The grey image is a monochromatic image represented by the 2D array, it simplifies data information and reduces the difficulty of analysis. The grey image is shown in Fig. 4c. Colour depth is divided into many levels between black and white, the range is much wider than the recognition range of human eyes. This factor ensured the accuracy of the analysis. The principle of converting the RGB colour image to a grey image is to remove the colour and hue of the image and display only the brightness of the image. Three components of the RGB image were calculated using the weighted summation method (Chen *et al*., 2021):

$$G_{ray} = 0.298R + 0.587G + 0.144B, \quad (3)$$

where: G_{ray} is the grey value of the image and R, G, and B are the red, green, and blue values of the colour image, respectively.

In the grey image of the grain pile, thresholding introduced some noise into the binary image because the edge distribution of the pixel value represented the soybean grain and the pixel value represented the pore overlap. This noise was generated for the most part at the pore-particle interface, it was a manifestation of micropores or small particles within the pores. In order to reduce the presence of noise, morphological filters were applied to all of the threshold images. The filtering operation included two continuous applications, that is, using the same morphological structure elements for both the erosion and expansion operations to detect, modify, or delete some shape features in the image under consideration. In this operation, the entire image was made up of structural elements of the same size corresponding to the noise feature size.

The image contrast was enhanced by adding or subtracting the top-hat and bottom-hat transforms. The top-hat and bottom-hat transforms can be used to correct the effect caused by uneven illumination, where the top-hat transform is used for lighter objects against darker backgrounds, and the bottom-hat transform is used for darker objects against lighter backgrounds. The top-hat transform is used to enhance the edge information of the target by emphasizing the grey peak value of the image. The bottom-hat transform is used to find the valley value of the image and highlight the connection boundary between the image targets. The principle of the high-hat transformation is to select the structural elements and subtract the image produced by the morphological operation from the original image, thus changing the image background and enhancing the image contrast. All of the grain pile slice images were normalized in order to reduce the impact of the pixel differences between the adjacent grain pile slice images.

Image segmentation is the process of separating each pixel of an image into any one of two or more sets (Robertson and Campbell, 1997). In order to observe and analyse images more intuitively, the image information is converted into binary information that is easier to analyse. Binary images are 2D arrays of 0 (black) and 1 (white). This image-processing method makes the recognition of image information easier. In this study, all of the slice images were segmented based on their threshold value, which separated the pixels belonging to the blue colour channel (resin-filled holes) and particles to generate a binary image with a particle strength value of 1 (white) and a pore strength value of 0 (black) in the image, as shown in Fig. 4d. If the original image is $F(x, y)$ and the threshold is T, the principle of image binarization will be as follows:

$$G(x,y)=\begin{cases}1 & F(x,y)\geq T\\ 0 & F(x,y)<T\end{cases}, \tag{4}$$

where: $F(x, y)$ is the pixel value of a point in the image matrix and T is the threshold value. If it is less than the threshold value, the value is 0 and the rest are 1.

The key to binarization is to select the appropriate threshold for image segmentation. In this study, the method of the maximum variance between classes, which was constructed using ImageJ software, namely the Ostu algorithm, was adopted. This method is based on the principle of least squares and is statistically the best segmentation method. The grey value of an image is divided into two parts using the best threshold to maximize the variance of the parts. Part of the binary map was selected after image processing under 0, 100, 200, and 300 kPa, as shown in Fig. 5, in order to visually observe the effect of vertical pressure on the pore structure of the grain piles. Figure 5 shows that with an increase in vertical pressure, the number of pixels occupied by grain pile particles gradually increases, whereas the number of pixels occupied by pores gradually decreases.

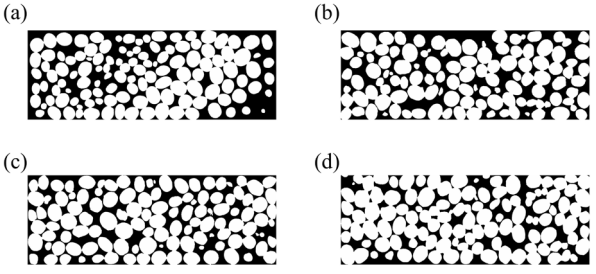

Fig. 5. Binary diagram of the grain pile under different vertical pressures: a – 0, b – 100, c – 200, and d – 300 kPa.

The initial porosity of the grain pile was calculated using the following equation (Kocabiyik *et al*., 2004):

$$\varepsilon_{t_0}=1-\rho_b/\rho_s, \tag{5}$$

where: ε_{t_0} is the initial value of the theoretical grain pile porosity, ρ_b is the initial density of the grain pile (kg m^{-3}), and ρ_s is the grain particle density (kg m^{-3}).

The theoretical value of grain pile porosity under different pressures can be measured using a grain pile compression test and it was calculated using the following formula:

$$\varepsilon_{t_i}=1-(1-\varepsilon_{t_0})h/(h-h_i), \tag{6}$$

where: ε_{t_i} is the theoretical value of the grain pile porosity under i-level pressure, h is the initial height of the grain pile (mm), and h_i is the descending height of the grain pile under i-level pressure (mm).

After binary processing, the grain pile structure information was stored in a 2D array. Each element in the array was 0 or 1, which represented the grain pile pore phase and solid particles, respectively. The image method grain pile porosity was calculated using the following formula:

$$\varepsilon_{i_i}=N_0/(N_0+N_1), \tag{7}$$

where: ε_{i_i} is the porosity of the grain pile as determined by the image method under i-level pressure, N_0 is the number of pixels occupied by the pores, and N_1 is the number of pixels of grain.

The change in grain pile porosity under different pressures may be expressed by porosity variability, and its evaluation index is the relative difference between the porosity values. Compared with the porosity of the grain pile under a natural accumulation state, it can directly reflect the influence of pressure on porosity. The variation in porosity was calculated using the following formula:

$$E = (\varepsilon_{i_0} - \varepsilon_{i_i}) / \varepsilon_{i_0}, \quad (8)$$

where: E is the porosity variability and ε_{i_0} is the initial porosity of the grain pile using the image method under an i-level pressure.

The pore complexity can be quantitatively evaluated by using the fractal dimension. In a 2D case, the perimeter and area of a regular graph conform to the following relationship:

$$C \propto A^{\frac{1}{2}}, \quad (9)$$

where: C is the perimeter of the 2D figure (cm), and A is the 2D graphic area (cm^2).

For irregular shapes, the fractal perimeter can be used to replace the actual perimeter in Eq. (9). The relationship between the fractal perimeter and area is as follows (Florio *et al*., 2019):

$$C(\varepsilon) \propto \left[A(\varepsilon)\right]^{\frac{D}{2}}, \quad (10)$$

where: ε is the measurement scale and $C(\varepsilon)$ and $A(\varepsilon)$ are the perimeter and area measured using this scale, respectively. Therefore, the fractal dimension D may be obtained by collecting the C and A values of the different measurement scales, and then drawing the lg$C$-lg$A$ curves. In practice, only one scale is used to measure the relevant information of the graph, and hence the C and A values under other scales are missing. Therefore, the following formula is often used to approximate the calculation of D (Rabbi *et al*., 2018):

$$D = 2 \times \lg C / \lg A, \quad (11)$$

where: D is the fractal dimension.

The ANOVA was carried out using SPSS statistical software in order to test for the effect of vertical pressure and horizontal position on the measured pore characteristics (porosity, pore area, pore diameter, fractal dimension).

RESULTS AND DISCUSSION

Based on the grain slice image and image processing technology, the porosity of the grain pile under different pressures was calculated, and the theoretical value of grain pile porosity under the same conditions was calculated through the performance of a compression test. The contrast diagram of grain pile porosity through the use of both image and theoretical methods under different pressures is shown in Fig. 6.

Figure 6 shows that under different pressures, the change trend in the grain pile porosity value is basically consistent with the theoretical value as determined using the image method. However, differences were observed in the grain pile porosity value, the maximum difference was 0.0087 and the relative error was 2.2%. In general terms, the results obtained using the image method may be applied to better reflect the porosity change rule under different pressures in terms of both the numerical value and change trend. This shows the effectiveness of the image method used in this study to analyse the pore characteristic parameters and also proves the credibility of the results.

The porosity change in the soybean grain pile under different vertical pressures is shown in Fig. 7.

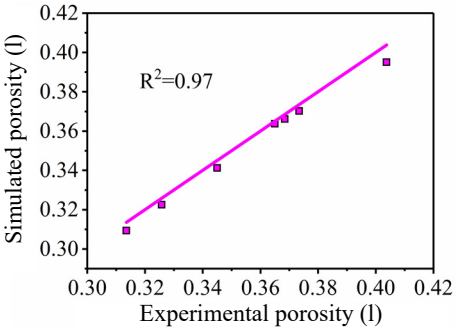

Fig. 6. Comparison between the porosity values of grain piles using both image and theoretical methods.

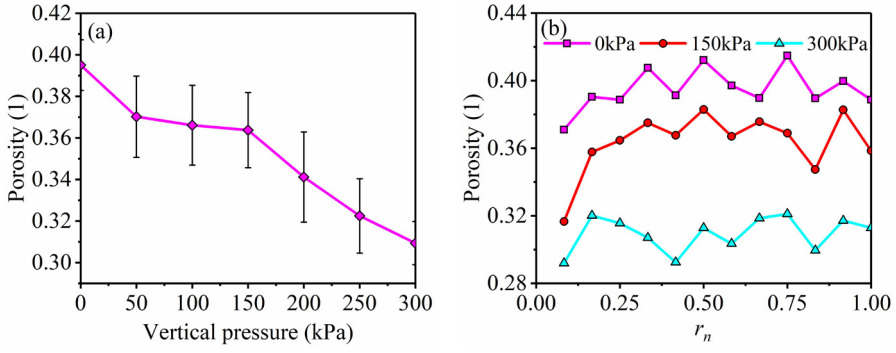

Fig. 7. Variation in the porosity of the grain pile under different vertical pressures: a – change in the overall average porosity and b – variation in porosity in the horizontal direction.

Figure 7a shows that with an increase in vertical pressure, the average porosity of the soybean grain pile gradually decreases. However, the change rule of the average porosity of the grain pile under different pressures is different. The initial pressure was 0, that is, when the soybean pile was naturally scattered, the porosity of the grain pile reached its highest value, which is 0.395. When the vertical pressure was 50 kPa, the porosity of the grain pile decreased rapidly to 0.3702, and the reduction in porosity under a unit pressure was 0.05%. Khatchatourian and Savicki (2004) conducted a study concerning the parameters of storing soybean grain piles in a lab-scale polyvinyl chloride bin with a diameter of 0.2 m and a height of 1.0 m. The results showed that the porosity of the soybean grain piles was 0.39, which is basically consistent with the research data obtained in this study. When the vertical pressure was 50-150 kPa, the porosity of the grain pile only decreased from 0.3702 to 0.3637, and the porosity decreased by 0.007% under unit pressure, also, the porosity changed slowly. When the vertical pressure was 150-300 kPa, the porosity change rate of the grain pile increased, the porosity of the grain pile decreased from 0.3637 to 0.3094, and the porosity reduction under unit pressure was 0.036%. When the vertical pressure is 0-250 kPa, the porosity of the grain pile decreases from 0.395 to 0.3225, with a change rate of 18.35%. The results of this study are basically consistent with the results reported by Liu *et al*. (2022d), that is, when the vertical pressure is 0-250 kPa, the porosity change rate of the grain piles is 18.6%. Overall, with increases in vertical pressure, the porosity change rate of the grain pile presented an S-shaped change rule of fast in the front, slow in the middle, and fast in the rear. The reason for this change is that under the state of natural accumulation, the grain pile is loose and the contact points between the particles are lower. After bearing a certain pressure, the particles in the unstable state move downward. Because the particles are in an unstable state, the pressure increment required to produce a certain amount of displacement is small and hence the porosity value decreases rapidly under pressure. Subsequently, the number of contact points between the particles increases, this results in an increased compressive resistance and a slow change in porosity. Due to the high degree of sphericity of the soybean particles, most of them are concentrated in the range above 0.90, which is considered to be approximately spherical, and the distribution of the equivalent diameter is also relatively concentrated, accounting for 85% of the particles between 7.2-7.6 mm. The accumulation situation is similar to that of an isodiametric sphere. When the applied pressure continues to increase, it may cause changes in the particle accumulation arrangement or in the elastic deformation of the particles, which results in a reduction in grain pile porosity. Thompson and Ross (1983) studied the effect of compaction on the porosity of the grain piles, the results indicated that the porosity of the grain piles decreased with increases in vertical pressure, this may be due to the rearrangement of the grain particles, which is consistent with the results of this study.

In order to further study changes in the rules governing porosity under pressure, the changes in grain pile porosity along the horizontal direction at 0, 150, and 300 kPa were evaluated, and the results are shown in Fig. 7b. In this figure, $r_n = r_i/R$ is the dimensionless distance from the wall, r_i is the distance from the horizontal position of the grain pile slice to the side wall of the grain pile casting body, and R is the distance from the horizontal side wall to the centre surface of the grain pile casting body. Figure 7b shows that under different vertical pressures, the grain pile porosity displayed a similar change trend along the horizontal direction, and the grain pile porosity oscillated along the horizontal direction from the side wall to the centre. With increases in vertical pressure, the porosity of the grain pile section at the same location gradually decreased, this was mainly due to an increase in grain pile particle volume and a decrease in the pore area caused by vertical pressure. Klerk (2003) obtained an empirical formula for predicting the porosity distribution in a cylindrical packed bed through performing experiments, and the results showed that the radial porosity oscillates in the direction towards the centre of the packed bed, which is consistent with the results of this study. Liu *et al*. (2022d) arrived at similar conclusions through the study of a discrete element packing model which was used to determine the radial porosity distribution of a cylindrical packed bed.

The results of the ANOVA analysis statistical tests on the porosity of the grain piles at different vertical pressures and horizontal positions are shown in Table 2. The results show that at the 0.05 level, both the vertical pressure and the horizontal position distribution have a significant impact on porosity.

Table 2. ANOVA results for the effect of the vertical pressure and horizontal position on porosity

Source	DF	SS	MS	F	Significance
Vertical pressure	0.06392	6	0.01065	64.76519	0.000
Horizontal position	0.01253	11	0.00114	6.92674	0.000
Error	0.01086	66	0.00016		
Total	0.08731	83			

DF – degree freedom, SS – stdey square, MS – mean square, F – joint hypothesis testing statistics.

Pore variability refers to the different degrees of grain pile porosity under different pressures. The change in grain pile porosity variability under different pressures is shown in Fig. 8.

Figure 8 shows that with an increase in vertical pressure, the porosity of the grain pile decreases, and the variability in its porosity gradually increases. When the vertical pressure was 50 kPa, the grain pile variability was 6.49%. When the vertical pressure was 50-150 kPa, the grain pile variability decreased by 1.8%. When the vertical pressure was 150-300 kPa, the grain pile variability increased significantly, and its value increased from 8.25 to 24.33%. The porosity variation of the grain pile was closely related to porosity, which reflected the degree of difference in the porosity under different pressures. This study compares the porosity of the grain piles at natural state (0 kPa) conditions, so this value can directly reflect the influence of pressure on porosity.

Figure 9 shows the change in the pore area of the soybean grain pile under different vertical pressures. Figure 9a shows that with an increase in vertical pressure, the average pore area of the soybean grain pile decreases gradually, but the change rule of the average pore area of the grain pile is different under different pressures. The initial pressure was 0, that is, under the natural scattering state of the soybean pile, the average pore area of the grain pile reached its highest value, which is 0.0864 cm^2. When the vertical pressure was 50 kPa, the average pore area of the grain pile decreased rapidly to 0.0807 cm^2, and the average pore area change rate under unit pressure was 0.011%. When the vertical pressure was 50-150 kPa, the average pore area of the grain pile decreased from 0.0807 cm^2 to 0.0769 cm^2. The average pore area changed slowly, and the average pore area change rate under unit pressure was 0.004%. When the vertical pressure was 150-300 kPa, the average pore area change rate of the grain pile increased, the average pore area of the grain pile decreased from 0.0769 cm^2 to 0.0571 cm^2, and the average pore area change rate under unit pressure was 0.014%. In its natural accumulation state, the grain pile is loose, the number of macropores between the grains is large, and the average pore area of the grain pile is large. Under minor pressure, the particles with less contact will be the first to move closer. Because there are few contact points between the particles at this time, the pore area decreases rapidly under pressure. Subsequently, the proportion of the particles in contact with each other increases, the resulting compressive resistance increases, and the main sliding displacement between the particles causes the rate of change in pore area to decrease. With an increase in vertical pressure, when the particles continue to move closer together, there will be sliding and even rotation, this results in a further reduction in the grain pile pore area. Huang *et al*. (2013) extracted a three-dimensional pore network model of the soybean and corn grain piles, thereby indicating that the pore volume gradually decreases with an increase in vertical pressure, which is consistent with the results of this study.

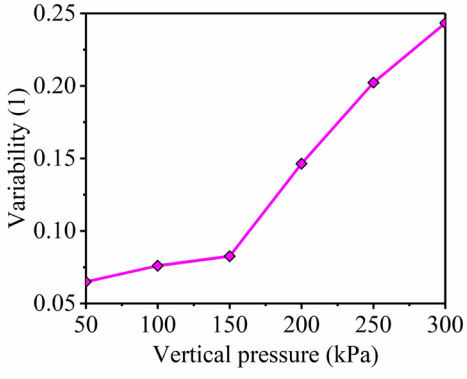

Fig. 8. Variation in grain pile porosity under different pressures.

In order to further study the variation in pore area with pressure, the variation in grain pile pore area along the horizontal direction at 0, 150, and 300 kPa was assessed, and the results are shown in Fig. 9b. Under different vertical pressures, the distribution of the grain pile pore area along the horizontal direction from the side wall to the centre was quite different. With an increase in vertical pressure, the pore area of the grain pile section at the same location gradually decreased.

The results of ANOVA analysis statistical tests on the pore area of the grain piles at different vertical pressures and horizontal positions are shown in Table 3. The results

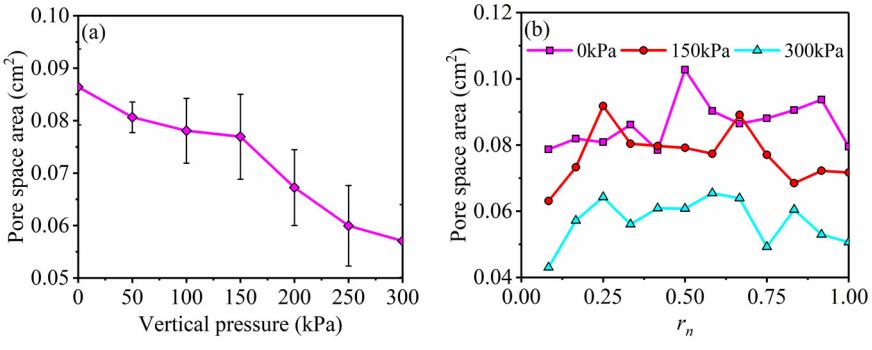

Fig. 9. Variation in the grain pile pore area under different vertical pressures: a – changes in the overall average pore area and b – variation in the pore area in a horizontal direction.

Table 3. ANOVA results from the effect of the vertical pressure and horizontal position on the pore area

Source	DF	SS	MS	F	Significance
Vertical pressure	0.00881	6	0.00147	48.93332	0.000
Horizontal position	0.00158	11	0.00014	4.78430	0.00002
Error	0.00198	66	0.00003		
Total	0.01237	83			

Explanations as in Table 2.

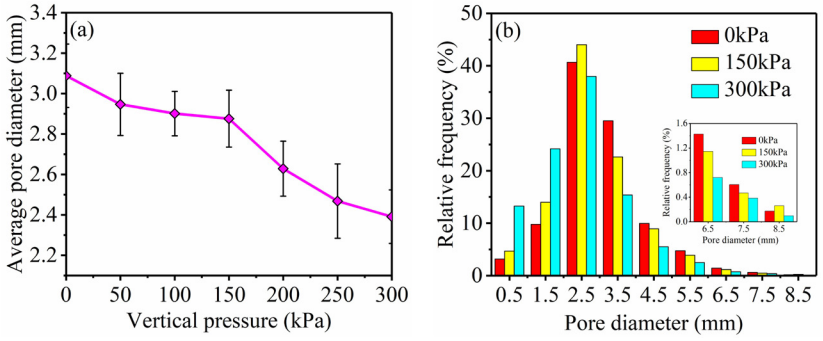

Fig. 10. Variation in the pore diameter of the grain pile under different vertical pressures: a – change in the overall average pore diameter and b – variation in the pore diameter in the horizontal direction.

show that at the 0.05 level, both the vertical pressure and horizontal position distribution have a significant impact on the pore area.

In order to facilitate the statistics of pore information and the use of pore size determination to characterize pore size, this study made use of the equivalent circular area, instead of pore area, in order to obtain an equivalent circular diameter, namely a pore diameter (Fu and Yu, 2019; Kang *et al*., 2018). Figure 10 shows the pore diameter change in the grain pile under different vertical pressures. Figure 10a shows that the average diameter of the grain pile decreases with an increase in pressure. The initial pressure was 0, that is, when the soybean pile is naturally scattered, the average pore diameter of the grain pile reached its highest point, which is 3.09 mm. When the vertical pressure was 50 kPa, the average pore diameter of the grain pile decreased rapidly to 2.95 mm, and the rate of change in the average pore diameter under unit pressure was 0.28%. When the vertical pressure was 50-150 kPa, the average pore diameter of the grain pile decreased from 2.95 to 2.88 mm, the average pore diameter changed slowly, and the average pore diameter change rate under a unit pressure was 0.07%. When the vertical pressure was 150-300 kPa, the average diameter change rate of the grain pile pore increased, the average diameter of the grain pile pore decreased from 2.88 to 2.39 mm, and the average diameter change rate of the grain pile pore under a unit pressure was 0.33%. With increases in the vertical pressure, the average pore diameter of the soybean grain pile gradually decreases, which is consistent with the results obtained by Huang *et al*. (2013).

The characterization of pores in terms of their quantity, shape, and size is relatively complex, and it is difficult to demonstrate the size distribution rule using a single mean or extreme value analysis. In order to further study the influence of pressure on the distribution of the grain pile pore diameter, the proportions of the different grain pile pore diameters at 0, 150, and 300 kPa were examined. Figure 10b shows the change in the proportion of the grain pile pore diameter under different vertical pressures. The proportion of the various grain pile pore diameters varied under different pressures, but pores with a diameter of 0.5-3.5 mm formed the largest category of pores, and the proportion of the grain pile pore diameter at 0, 150, and 300 kPa was found to be 83.10, 85.29, and 90.80%, respectively. Huang *et al*. (2013) studied the changes in pore structure under different grain pile heights, and the results showed that the largest proportion of the soybean pore radius present was 0.5-1.95 mm. They also found that when the pile height increased, the pressure on the grain pile increased, and the proportion of the small pore diameter also increased, which is consistent with the results of this study. With an increase in vertical pressure, the proportion of the pore diameter in the range of < 2.5 mm gradually increased, whereas the proportion of the pore diameter in the range of > 2.5 mm gradually decreased. Robertson and Campbell (1997) obtained similar results in their experiments, which revealed that the vertical pressure narrows the pore space, resulting in a decrease in the number of pores with large diameters and an increase in the number of pores with small diameters.

Table 4. ANOVA results for the effect of the vertical pressure and horizontal position on the pore diameter

Source	DF	SS	MS	F	Significance
Vertical pressure	4.96825	6	0.82804	58.14500	0.000
Horizontal position	0.61099	11	0.05554	3.90068	0.00023
Error	0.93982	66	0.01424		
Total	6.51906	83			

Explanations as in Table 2.

The results of ANOVA analysis statistical tests on the pore diameter of the grain piles at different vertical pressures and horizontal positions are shown in Table 4. The results show that at a 0.05 level, both the vertical pressure and the horizontal position distribution have a significant impact on the pore diameter.

Grain pile porosity is an irregular structure. The process of finding quantitative indicators to accurately describe its complexity is necessary. The fractal dimension describes the similar characteristics of the grain pile pores, and is a comprehensive reflection of the irregular grain pile pore size and the contact boundary between the pores and the grain particles. It can be used to characterize the complexity of the grain pile pore structure, which is related to the pore shape.

Figure 11 shows the changes in the pore fractal dimension of the soybean grain pile under different vertical pressures. With an increase in vertical pressure, the average pore fractal dimension of the whole soybean grain pile gradually increased. When the vertical pressure was 0-300 kPa, the average pore fractal dimension of the grain pile increased from 1.35 to 1.50, with a change rate of 10%. As the vertical pressure increased, the compactness of the soybean accumulation increased. An increase in the number of indirect contact points between the particles led to an increase in the number of elongated and irregular pores, and also the pore shape became complex. The more complex the pore shape is, the larger the circumference of the pores with the same area size, that is, the larger the overall fractal dimension of the pores. In order to further study the variation in the pore fractal dimension with pressure, the variation in the grain pile fractal dimension along the horizontal direction at 0, 150, and 300 kPa was studied, and the results are shown in Fig. 11b. Under different vertical pressures, the distribution of the fractal dimension of the grain pile pores along the horizontal direction from the side wall to the centre varied. With an increase in vertical pressure, the fractal dimension of the grain pile at the same location increased. Similar results were obtained by Neethirajan and Jayas (2007), who found that the complexity of the soybean pore shapes varies greatly along the horizontal direction. This study shows that the pressure effect does not reduce the complexity difference of the grain pile pore shapes.

The results of ANOVA analysis statistical tests on the fractal dimension of the grain piles at different vertical pressures and horizontal positions are shown in Table 5.

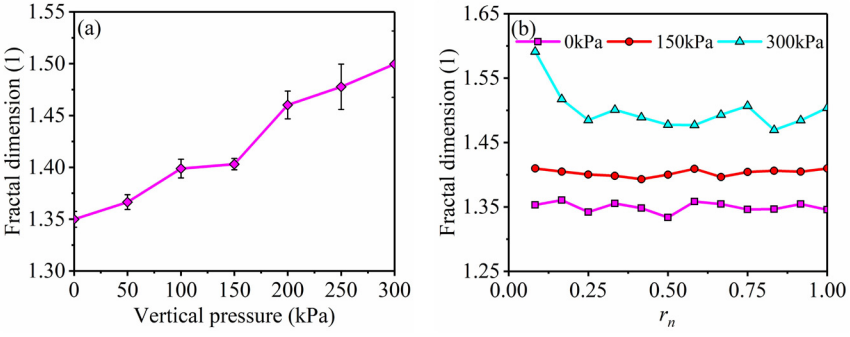

Fig. 11. Fractal dimension change in grain pile pores under different vertical pressures: a – change in the overall average pore fractal dimension and b – variation in the fractal dimensions of pores in the horizontal direction.

Table 5. ANOVA results for the effect of vertical pressure and the horizontal position on the fractal dimension

Source	DF	SS	MS	F	Significance
Vertical pressure	0.23696	6	0.03949	193.90337	0.000
Horizontal position	0.00750	11	0.00068	3.34767	0.00104
Error	0.01344	66	0.00020		
Total	0.25790	83			

Explanations as in Table 2.

The results show that at the 0.05 level, both the vertical pressure and the horizontal position distribution have a significant impact on the fractal dimension.

CONCLUSIONS

This study aimed to analyse the influence of the vertical pressure on the pore structure characteristics of the grain piles in the grain storage environment of large storage structures. In this study, grain casting section and image processing technology were used to study the change rule of vertical pressure on the pore structure parameters of a bulk soybean grain pile. The main conclusions are as follows:

1. Under different vertical pressures, the grain pile porosity values and variation trends revealed by the image and theoretical methods are basically consistent. With an increase in vertical pressure, the porosity in the grain pile decreases, and presents an S-shape with a fast front, slow middle, and fast rear. The porosity of the grain piles is significantly affected by both the vertical pressure and horizontal position. The porosity variability in the grain pile gradually increases with the increase in vertical pressure.

2. With the increase in vertical pressure, the pore area and diameter of the grain pile gradually decreased, and this was significantly affected by the horizontal position. The proportion of the grain pile pore diameter varied under different pressures, but the pores with a pore diameter of 0.5-3.5 mm occupied the largest portion. With the increase in vertical pressure, the proportion of the aperture in the range of < 2.5 mm gradually increased, whereas the proportion of the aperture in the range of > 2.5 mm gradually decreased.

3. With an increase in vertical pressure, the average fractal dimension of the pores in the soybean grain piles increased gradually. When the vertical pressure was 0-300 kPa, the average fractal dimension change rate of the grain pile pore was 10%. The fractal dimension was significantly influenced by the horizontal position. Under various vertical pressures, the distribution of the fractal dimension of the grain pile pores along the horizontal direction from the side wall to the centre was different. With an increase in the vertical pressure, the fractal dimension of the grain pile at the same location increases.

Conflict of interest: The authors declare no conflict of interest.

REFERENCES

ASAE S352.2 APR1988 (R2017), 2017. Moisture measurement-unground grain and seeds. ASAE: St. Joseph, Mich: USA.

ASAE D241.4 OCT1992 (R2017ED), 2017. Density, specific gravity, and mass-moisture relationships of grain for storage. ASAE: St. Joseph, Mich, USA.

Altuntas E. and Demirtola H., 2007. Effect of moisture content on physical properties of some grain legume seeds. New Zealand J. Crop Hort. Sci., 35(4), 423-433, https://doi.org/10.1080/01140670709510210.

Amanlou Y. and Zomorodian A.A., 2011. Resistance to air flow across a thin green fig bed. J. Agric. Sci. Technol., 13(5), 677-685.

Budhathoki S., Lamba J., Srivastava P., Malhotra K.,Way T.R. and Katuwal S., 2022. Using X-ray computed tomography to quantify variability in soil macropore characteristics in pastures. Soil Till. Res., 215, 105194, https://doi.org/10.1016/j.still.2021.105194.

Chen G.L., Li F.L., Geng J.Y., Jing P.F. and Si Z.K., 2021. Identification, generation of autoclaved aerated concrete pore structure and simulation of its influence on thermal conductivity. Construction Building Materials, 294, 123572 https://doi.org/10.1016/j.conbuildmat.2021.123572.

Chen P., Huang K., Wang F., Xie W., Wei S., and Yang D., 2019. Simulation of heat and mass transfer in a grain pile on the basis of a 2D irregular pore network. Fluid Dynamics Materials Proc., 15(4), 367-389, https://doi.org/10.32604/fdmp.2019.07762.

Cheng X.D., Zhang Q., Shi C.X., and Yan X.J., 2017. Model for the prediction of grain density and pressure distribution in hopper-bottom silos. Biosys. Eng., 163, 159-166, https://doi.org/10.1016/j.biosystemseng.2017.09.006.

Cheng X.D., Zhang Q., Yan X.J., and Shi C.X., 2015. Compressibility and equivalent bulk modulus of shelled corn. Biosystems Engineering, 140, 91-97, https://doi.org/10.1016/j.biosystemseng.2015.10.001.

Chung D.S., Maghirang R.G., Kim Y.S., and Kim M.S., 2001. Effects of moisture and fine material on static pressure drops in a bed of grain sorghum and rough rice. Trans. ASAE, 44(2), 331-336, https://doi.org/10.13031/2013.4667.

Florio B.J., Fawell P.D., and Small M., 2019. The use of the perimeter-area method to calculate the fractal dimension of aggregates. Powder Technol., 343, 551-559, https://doi.org/10.1016/j.powtec.2018.11.030.

Fu J. and Yu Y., 2019. Experimental study on pore characteristics and fractal dimension calculation of pore structure of aerated concrete block. Advances Civil Eng., 8043248, https://doi.org/10.1155/2019/8043248.

Ghodki B.M., Patel M., Namdeo R., and Carpenter G., 2019. Calibration of discrete element model parameters: soybeans. Computational Particle Mechanics, 6(1), 3-10, https://doi.org/10.1007/s40571-018-0194-7.

Haque E., 2011. Void fraction as a function of depth and pressure drops of packed beds of porous media formed by granular materials. Trans. ASABE, 54(6), 2239-2243, https://doi.org/10.13031/2013.40636.

Hilton J.E., Mason L.R., and Cleary P.W., 2010. Dynamics of gas-solid fluidised beds with non-spherical particle geometry. Chem. Eng. Sci., 65(5), 1584-1596, https://doi.org/10.1016/j.ces.2009.10.028.

Hu W.L., Jiang Y., Chen D.Y., Lin Y.S., Han Q., and Cui Y.F., 2018. Impact of pore geometry and water saturation on gas effective diffusion coefficient in soil. Applied Sciences-Basel, 8(11), https://doi.org/10.3390/app8112097.

Huang K., Wang X., Liu X., Wang X., and Yang D., 2013. Construction of Three-Dimensional Pore Network in Bulk Grain. Drying Technol., 31(15), 1871-1878, https://doi.org/10.1080/07373937.2013.834927.

Kang S.H., Hong S.G., and Moon J., 2018. The effect of superabsorbent polymer on various scale of pore structure in ultra-high performance concrete. Construction Building Materials, 172, 29-40, https://doi.org/10.1016/j.conbuildmat.2018.03.193.

Khatchatourian O.A. and Savicki D.L., 2004. Mathematical modelling of airflow in an aerated soya bean store under non-uniform conditions. Biosystems Eng., 88(2), 201-211, https://doi.org/10.1016/j.biosystemseng.2004.03.001.

Klerk A. de, 2003. Voidage variation in packed beds at small column to particle diameter ratio. AIChE J., 49(8), 2022-2029, https://doi.org/10.1002/aic.690490812.

Kocabiyik H., Aktas T., and Kayisoglu B., 2004. Porosity rate of some kernel crops. J. Agronomy, 3(2), 76-80, https://doi.org/10.3923/ja.2004.76.80.

Lawrence J. and Maier D.E., 2012. Prediction of temperature distributions in peaked, leveled and inverted cone grain mass configurations during aeration of corn. Appl. Eng. Agric.,28(5),685-692,https://doi.org/10.13031/2013.42419.

Lawrence J., Maier D.E., and Stroshine R.L., 2013. Three-dimensional transient heat, mass, momentum, and species transfer in the stored grain ecosystem: part I. model development and evaluation. Trans. ASABE, 56(1), 179-188, https://doi.org/10.1016/j.protcy.2013.11.092.

Liu B.Q., Zhang X.H., Wang L.G., and Hong H., 2008. Fluidization of non-spherical particles: sphericity, zingg factor and other fluidization parameters. Particuology, 6(2), 125-129, https://doi.org/10.1016/j.cpart.2007.07.005.

Liu C.S., Chen G.X., Zhou Y., Yuel L.F., and Liu W.L., 2022a. Investigation on compression and mildew of mixed and separated maize. Food Sci. Nutr., https://doi.org/10.1002/fsn3.2985.

Liu C.S., Chen G.X., Zhou Y., Zheng D.Q., and Zhang Z.J., 2022b. Element tests and simulation of effects of vertical pressure on compression and mildew of wheat. Computers Electronics Agric., 203, 107447, https://doi.org/10.1016/j.compag.2022.107447.

Liu C.S., Zhou Y., Chen G.X., Zheng D.Q. and Yue L.F., 2022c. Compression and fungal heat production in maize bulk considering kernel breakage. Applied Sciences-Basel, 12(10), 4870, https://doi.org/10.3390/app12104870.

Liu W.L., Chen G.X., Liu C.S., Zheng D.Q., and Ge M.M., 2022d. Experimental and numerical study of pressure drop characteristics of soybean grain under vertical pressure. Appl. Sciences-Basel, 12(14), 6830, https://doi.org/10.3390/app12146830.

Mohapatra D., Kumar S., Kotwaliwale N., and Singh K.K., 2017. Critical factors responsible for fungi growth in stored food grains and non-Chemical approaches for their control. Industrial Crops Products, 108, 162-182, https://doi.org/10.1016/j.indcrop.2017.06.039.

Nalladurai K., Alagusundaram K., and Gayathri P., 2002. PH-postharvest technology: airflow resistance of paddy and its byproducts. Biosys. Eng., 83(1), 67-75, https://doi.org/https://doi.org/10.1006/bioe.2002.0091.

Narendran R.B., Jian F.J., Jayas D.S., Fields P.G., and White N.D.G., 2019. Segregation of canola, kidney bean, and soybean in wheat bulks during bin loading. Powder Technol., 344, 307-313, https://doi.org/10.1016/j.powtec.2018.12.042.

Neethirajan S., Jayas D.S., White Ndg and Zhang H., 2008. Investigation of 3D geometry of bulk wheat and pea pores using x-ray computed tomography images. Computers Electronics Agric., 63(2), 104-111, https://doi.org/10.1016/j.compag.2008.01.019.

Neethirajan S., Karunakaran C., Jayas D.S., and White Ndg, 2006. X-ray Computed Tomography Image Analysis to explain the Airflow Resistance Differences in Grain Bulks. Biosys. Eng., 94(4), 545-555, https://doi.org/10.1016/j.biosystemseng.2006.04.013.

Neethirajan S. and Jayas D.S., 2007. Analysis of pore network in three-dimensional (3D) grain bulks using x-ray CT images. Transport in Porous Media, 73(3), 319-332, https://doi.org/10.1007/s11242-007-9172-x.

Nourmohamadi-Moghadami A., Zare D., Singh C.B., and Stroshine R.L., 2020a. Filling of a grain silo. Part 1: Investigation of fine material distribution in a small scale centre-filled silo. Biosystems Engineering, 191, 145-156, https://doi.org/10.1016/j.biosystemseng.2020.01.003.

Nourmohamadi-Moghadami A., Zare D., Stroshine R.L., and Kamfiroozi S., 2020b. Filling of a grain silo. Part 2: A new filling method for uniform distribution of fines in a small scale silo. Biosys. Eng., 191, 157-167, https://doi.org/10.1016/j.biosystemseng.2020.01.001.

Nwaizu C. and Zhang Q., 2021. Computational modeling of heterogenous pore structure and airflow distribution in grain aeration system. Computers Electronics Agric., 188, 106315, https://doi.org/10.1016/j.compag.2021.106315.

Olatunde G., Atungulu G.G., and Sadaka S., 2016. CFD modeling of air flow distribution in rice bin storage system with different grain mass configurations. Biosys. Eng., 151, 286-297, https://doi.org/10.1016/j.biosystemseng.2016.09.007.

Panigrahi S.S., Singh C.B., and Fielke J., 2020. CFD modelling of physical velocity and anisotropic resistance components in a peaked stored grain with aeration ducting systems. Computers Electronics Agric., 179, https://doi.org/10.1016/j.compag.2020.105820.

Rabbi S.M.F., Tighe M.K., Flavel R.J., Kaiser B.N., Guppy C.N., Zhang X.X., and Young I.M., 2018. Plant roots redesign the rhizosphere to alter the three-dimensional physical architecture and water dynamics. New Phytologist, 219(2), 542-550, https://doi.org/10.1111/nph.15213.

Shedd C.K., 1951. Some new data on resistance of grains to airflow. Agric. Eng., 32(9), 493-495.

Thompson S.A. and Ross I.J., 1983. Compressibility and frictional coefficients of wheat. Trans. ASAE, 26(4), 1171-1176, https://doi.org/10.13031/2013.34099.

Tian W. and Han N., 2018. Pore characteristics (> 0.1 mm) of non-air entrained concrete destroyed by freeze-thaw cycles based on CT scanning and 3D printing. Cold Regions Science Technol., 151, 314-322, https://doi.org/10.1016/j.coldregions.2018.03.027.

Tiusanen M., Jokiniemi J., and Hautala M.I., 2013. Grain dryer temperature optimisation with simulation and a test dryer. IFAC Proc. Volumes, 46(18), 12-17, https://doi.org/https://doi.org/10.3182/20130828-2-SF-3019.00025.

Vicente M.A., Gonzalez D.C., and Minguez J., 2019. Recent advances in the use of computed tomography in concrete technology and other engineering fields. Micron, 118, 22-34, https://doi.org/10.1016/j.micron.2018.12.003.

Vicente M.A., Gonzalez D.C., Minguez J., Tarifa M.A., Ruiz G., and Hindi R., 2018. Influence of the pore morphology of high strength concrete on its fatigue life. Int. J. Fatigue, 112, 106-116, https://doi.org/10.1016/j.ijfatigue.2018.03.006.

Sobieski W., Zhang Q., and Liu C., 2012. Predicting tortuosity for airflow through porous beds consisting of randomly packed spherical particles. Transport in Porous Media, 93(3), 431-451, https://doi.org/10.1007/s11242-012-9961-8.

Wu Z.D., Zhang Q., Yin J., Wang X.M., Zhang Z.J., Wu W.F., and Li F.J., 2020. Interactions of mutiple biological fields in stored grain ecosystems. Sci. Reports, 10(1), 9302, https://doi.org/10.1038/s41598-020-66130-6.

Yuan J., Wu Y., and Zhang J.K., 2018. Characterization of air voids and frost resistance of concrete based on industrial computerized tomographical technology. Construction Building Materials, 168, 975-983, https://doi.org/10.1016/j.conbuildmat.2018.01.117.

Yuan Y., Tan, L., Zhao Z., Xu Y., Zhao Y., and Yuan Y., 2016. Multiscale and multilayer structural modeling and simulation on drying of grain packing porous media. Drying Technol., 34(14), 1664-1676, https://doi.org/10.1080/07373937.2016.1141213.

Yue R. and Zhang Q., 2017a. A pore-scale model for quantifying airflow paths through grain bulks. Trans. ASABE, 60(3), 965-972, https://doi.org/https://doi.org/10.13031/trans.12032.

Yue R. and Zhang Q., 2017b. A pore-scale model for predicting resistance to airflow in bulk grain. Biosystems Eng., 155, 142-151, https://doi.org/10.1016/j.biosystemseng.2016.12.007.